Controlling pulse propagation in optical fibers through nonlinearity and dispersion management

Rajneesh Atre[1] and Prasanta K. Panigrahi[1]
[1]*Physical Research Laboratory, Navrangpura, Ahmedabad 380 009, India*
[2]*School of Physics, University of Hyderabad, Hyderabad-500 046, India*
(Received 16 December 2006; published 25 October 2007)

In the case of the nonlinear Schrödinger equation with designed group velocity dispersion, variable nonlinearity, and gain or loss, we analytically demonstrate the phenomenon of chirp reversal crucial for pulse reproduction. Two different scenarios are exhibited, where the pulses experience identical dispersion profiles, but show entirely different propagation behavior. Exact expressions for dynamical quasisolitons and soliton bound states relevant for fiber communication are also exhibited.

DOI: 10.1103/PhysRevA.76.043838 PACS number(s): 42.81.Dp, 05.45.Yv, 42.65.Tg

Nonlinear Schrödinger equation (NLSE) is known to govern the pulse dynamics in nonlinear optical fibers [1]. In recent years, the study of nonlinear fiber optics, dealing with optical solitons, has attracted considerable attention since it has an important role in the development of several technologies of the 21st century [2]. NLSE with distributed coefficients, such as group velocity dispersion (GVD), distributed nonlinearity, and gain or loss, is being studied extensively in order to determine the effect of various distributed parameters on the pulse profile.

In the realistic situation in a fiber, there arises nonuniformity due to variation in the lattice parameters of the fiber medium, as a result of which the distance between two neighboring atoms is not constant throughout the fiber. It may also arise due to the variation of the fiber geometry, e.g., diameter fluctuation. These nonuniformities influence effects, such as loss (or gain), phase modulation, etc., which can be modeled by making corresponding parameters space dependent. From a practical point of view, tailoring of various fiber parameters may lead to effective control of the pulse. This has been one of the prime motivations of a number of authors to analyze NLSE in a distributed scenario.

Dispersion management has emerged as an important technology to control and manipulate the light pulses in optical fibers [2,3]. Pulse compression has been demonstrated with appropriately designed GVD and nonlinearity in the presence of chirping [4–6], as also through soliton effects [7]. Adiabatic soliton compression, through the decrease of dispersion along the length of the fiber has been shown to provide good pulse quality [8]. The possibility of amplification of soliton pulses using a rapidly increasing distributed amplification with scale lengths comparable to the characteristic dispersion length has been reported [9]. It has been numerically shown that, in the case where the gain due to the nonlinearity and the linear dispersion balance each other, equilibrium solitons are formed [10]. Serkin and Hasegawa have formulated the effect of varying dispersion and other parameters on the soliton dynamics and have explained the concept of amplification of soliton [11].

The formal structure of the Lax pair for the deformed NLSE has been studied [12,13]. In a significant result, it has been numerically shown that in an appropriately designed dispersion profile chirped pulses can be retrieved through chirp reversal at a calculated location in the fiber [14]. The advantage of prechirping of the input pulse in overcoming soliton interaction and dispersive-wave generation has been noted earlier [16].

In the present paper, we demonstrate analytically the phenomenon of chirp reversal of quasisolitons with a designed dispersion profile. Very interestingly we find two possibilities of chirp reversal for which the dispersion profiles are identical. However, they exhibit entirely different propagation behavior. In one case the motion is sinusoidal and in the other case it shows pulse acceleration. The procedure to control pulse dynamics is also pointed out. Exact expressions for dynamical quasisolitons and soliton bound states relevant for fiber communication are exhibited.

It is worth emphasizing that, exact solutions have played a crucial role in demonstrating different pulse shaping techniques. The soliton solutions of NLSE or modifications of the same have come in handy in studying these mechanisms. In the same light, finding exact solutions for general types of distributed scenarios will illustrate the subtle effects and interplay of various parameters on formation and propagation dynamics of light pulses.

We develop a methodology to obtain self-similar solitary wave solutions of the generalized NLSE model with varying nonlinearity, GVD, gain or loss, and a confining oscillator which can be further modulated. One or a few of these parameters can be switched off depending on the situation at hand. It is shown that, this equation decouples into a elliptic function equation and a Schrödinger eigenvalue problem. This allows one to analytically treat a variety of distributed scenarios, a few of which we explicate in the text. In the context of Bose-Einstein condensates the procedure to deal with variable coefficient NLSE in the absence of GVD has been carried out recently by the present authors [17]. GVD leads to a fundamentally new control parameter in the present case dealing with optical fibers. For example, a subtle interplay of GVD and nonlinearity leads to a soliton bound state as will be seen below. The effect of GVD, alternating between normal and anomalous dispersion, on the pulse profile is also discussed.

For the purpose of analytic demonstration of chirp reversal we start with a NLSE model with variable GVD, nonlinearity, and loss or gain [14],

$$i\partial_z q(z,t) + \frac{d(z)}{2}\partial_{tt} q(z,t) + \gamma(z)|q|^2 q(z,t) + ig(z)q(z,t) = 0. \tag{1}$$

Following Ref. [14], here z and t are dimensionless. With $q(z,t)=a(z)u(z,t)$ and $a(z)=\exp[-\int_0^z dz' g(z')]$, one obtains

$$i\partial_{z'}u(z',t) + \frac{d_e(z')}{2}\partial_{tt}u(z',t) + \tilde{\gamma}(z')|u|^2u(z',t) = 0, \quad (2)$$

where $z' = \int_0^z dz'' a^2(z'')$, $d_e(z') = d(z)/a^2(z)$, and $\tilde{\gamma}(z') = \gamma(z)/a^2(z)$.

Keeping in mind, prechirping and the self-similar nature of the pulse we make use of the following ansatz:

$$u(z',t) = \sqrt{p(z')}\ \ \nu[p(z')t, z']\exp[iC(z')t^2], \quad (3)$$

where p and C are real functions of z'.

The numerical investigation of Kumar and Hasegawa [14] indicated that the soliton of the NLSE with distributed coefficients is intermediate between a sech and a Gaussian profile. This is our primary motivation to take into account the distributed coefficients through variable width and amplitude of the same sech profile. As will be shown, this self-similar ansatz leads to analytic solutions for a wide class of distributed coefficients.

However, in other scenarios the asymptotic and core functional dependencies of the profile can be different. An example of this kind can be found in Ref. [15].

Defining $\tau = p(z')t$, for preserving space-time identity, one obtains

$$i\left(\frac{\partial \nu}{\partial z'} + K_0\tau\frac{\partial \nu}{\partial \tau}\right) + \frac{d_e p^2}{2}\frac{\partial^2 \nu(z',\tau)}{\partial \tau^2} + \tilde{\gamma}(z')p|\nu|^2\nu(z',\tau) - \frac{K_1\tau^2 p}{2}\nu + \frac{iK_0\nu}{2} = 0, \quad (4)$$

where

$$K_0 = \frac{p_{z'} + Cd_e p}{p} \quad \text{and} \quad K_1 = \frac{C_{z'} + C^2 d_e}{p^3}. \quad (5)$$

We now tailor the dispersion profile with $K_0 = 0$ and $K_1 = \text{const}$,

$$i\frac{\partial \nu}{\partial z'} + \frac{d_e p^2}{2}\frac{\partial^2 \nu(z',\tau)}{\partial \tau^2} + \tilde{\gamma}(z')p|\nu|^2\nu(z',\tau) = \frac{K_1\tau^2 p}{2}\nu. \quad (6)$$

In order to map the above equation to one with constant anomalous dispersion we assume the constraint $d_e p = 1$ to obtain

$$i\frac{\partial \nu}{\partial z''} + \frac{1}{2}\frac{\partial^2 \nu(z'',\tau)}{\partial \tau^2} + \tilde{\gamma}(z'')|\nu|^2\nu(z',\tau) = \frac{K_1\tau^2}{2}\nu, \quad (7)$$

where $z'' = \int_0^{z'} p(s)ds$.

As mentioned earlier, the above equation has been numerically investigated, where a chirp reversal was observed for a quasisoliton having a profile intermediate to a Gaussian and the fundamental NLSE soliton [14]. These are stationary solutions obeying NLSE with an additional oscillator term, which explains the above profile. The exact solutions of Eq. (7) can be obtained following the formalism developed in Ref. [17]:

$$\nu(z'',\tau) = \sqrt{A(z'')}F\{A(z'')[\tau - \Lambda(z'')]\}e^{i\Phi(z'',\tau)}, \quad (8)$$

where

$$\Phi(z'',\tau) = a_1(z'') + b(z'')\tau - \frac{1}{2}c(z'')\tau^2. \quad (9)$$

Here, $a_1(z'') = a_{1_0} - \frac{\lambda-1}{2}\int_0^{z''} A^2(z)dz$, $\Lambda(z'') = \int_0^{z''} v(z)dz$, which satisfies the following equation:

$$\frac{d\Lambda}{dz''} + c(z'')\Lambda(z'') = b(z''), \quad (10)$$

with the general solution

$$\Lambda(z'') = \left(e^{-\int c(z'')dz''}\right)\left(\int dz''[b(z'')e^{\int c(z'')dz''}]\right). \quad (11)$$

The parameter $c(z'')$ obeys the Riccati equation

$$c_{z''} - c^2(z'') = K_1, \quad (12)$$

which can be exactly mapped to linear the Schrödinger eigenvalue problem. We also find the following consistency conditions:

$$\tilde{\gamma}(z') = \tilde{\gamma}_0 A(z')/A_0, \quad b(z'') = A(z''),$$

$$A(z'') = A_0\exp\left(\int_0^{z''} c(z)dz\right), \quad A_0 > 0. \quad (13)$$

F obeys the elliptic function equation in the new variable $T = A(z'')[\tau - \Lambda(z'')]$,

$$F''(T) - \lambda F(T) + 2\kappa F^3(T) = 0, \quad \text{where } \kappa = -\frac{\gamma_0}{A_0}. \quad (14)$$

The free real parameter λ, appearing in a_1 of Eq. (9), manifests in the above equation as the coefficient of the linear term. The 12 Jacobian elliptic functions satisfy the above equation and depend on the values of λ. These functions interpolate between the trigonometric and hyperbolic functions in the limiting cases [18]. Bright soliton solutions of the type $\nu(z'',\tau) = \sqrt{A(z'')}\,\text{sech}(T/T_0)e^{i\Phi(z'',\tau)}$ exist for $\kappa > 0$, where $T_0^2 = -A_0/\gamma_0$ and $\lambda = 1/2T_0^2$, similarly kink-type dark solitons exist for $\gamma_0 > 0$. We further note that, with normal dispersion one can obtain dark solitons for $\gamma_0 < 0$. It needs to be emphasized that, in the present approach the oscillator term leads to a dynamical chirp and modulates the pulse profile. However, the pulse retains its fundamental NLSE soliton character in the scaled variable z''.

Below, we examine the formation of bright quasi-soliton-like excitations, exhibiting chirp-reversal phenomenon. This

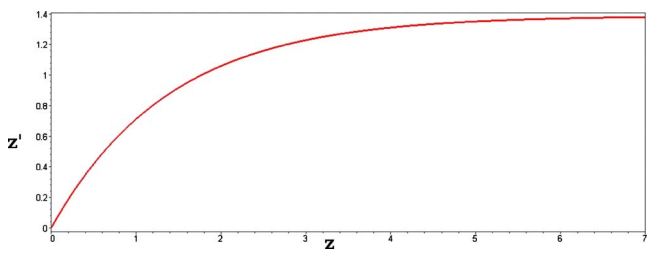

FIG. 1. (Color online) Variation of z' with physical parameter z. It is clear from the figure that as z increases z' saturates very fast.

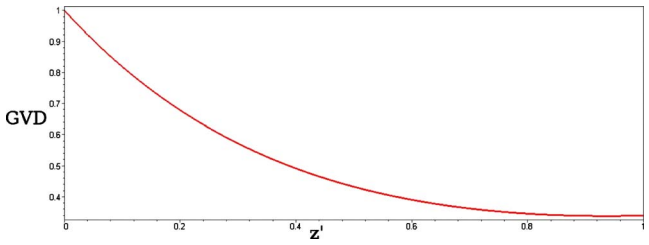

FIG. 2. (Color online) Variation of GVD with z' for parameter values $C(0)=-1.34$, $\Gamma=0.36$, and $K_1=1$.

is accomplished by the appropriate tailoring of GVD and prechirping of the launching pulse. Combining Eq. (5) and constraint $d_e p=1$ yield the following expressions for the tailored dispersion and the chirping parameter:

$$C=\frac{d_e'}{d_e^2} \quad \text{and} \quad d_e\frac{d^2d_e}{dz'^2}-\left(\frac{dd_e}{dz'}\right)^2=K_1. \tag{15}$$

It is interesting to notice that the choice of the constant K_1, gives rise to two scenarios, having identical dispersion and chirp profiles, but possessing entirely different pulse velocities.

We list below some explicit examples, depicting a variety of control mechanisms for pulse manipulation.

Soliton pulses exhibiting chirp reversal. Inspired from the numerical investigations of Kumar and Hasegawa [14], we first consider in Eq. (15), $K_1>0$, which is equivalent to a regular oscillator potential in Eq. (7). For constant loss $g(z)=\Gamma$, the dispersion profile reads as

$$d_e(z')=\cosh(\delta z')+\frac{C(0)}{\delta}\sinh(\delta z'), \tag{16}$$

$$d(z)=\exp(-2\Gamma z)\left(\cosh(\delta z')+\frac{C(0)}{\delta}\sinh(\delta z')\right)$$
$$\text{with} \quad \delta=[K_1+C^2(0)]^{1/2}. \tag{17}$$

It is worth pointing out that, the dispersion profile given by Eq. (16) is in the variable z'; since z' saturates very fast as z increases, behavior of GVD with respect to the physical variable z does not differ much from that of z'. We have plotted

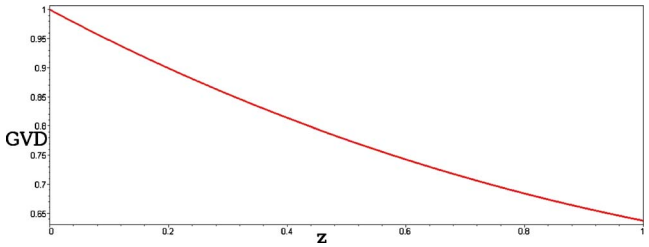

FIG. 3. (Color online) Variation of GVD with physical parameter z for the same parameter values as Fig. 2.

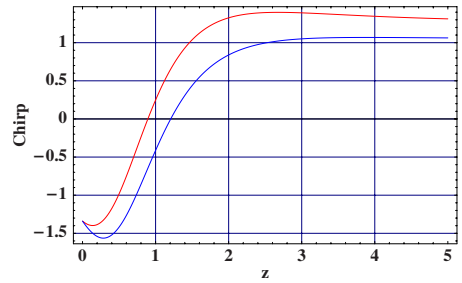

FIG. 4. (Color online) Depiction of the variation of chirp parameters with z. The top (red) curve shows the launching chirp and the bottom (blue) curve shows the same in combination with the dynamical chirp.

in Fig. 1, the variation of z' showing the above-mentioned saturation. We have also compared the behavior of GVD with respect to the parameter z' and the physical variable z in Figs. 2 and 3, respectively.

From the above dispersion profile we compute the launched chirp parameter $C(z')$ and plot it together with the dynamical chirp in Fig. 4. The top curve depicts the spatial evolution of the launching chirp and the bottom one that of launching and dynamical chirp together. From Eqs. (5) and (16) it is clear that launched chirp profile changes sign at $z(z_c')=(1/\delta)\tanh^{-1}[-C(0)/\delta]$.

The expression for the traveling quasisoliton, propagating with velocity $v(z'')=A_0\cos(K_0 z'')$, reads as

$$q(z,t)=a(z)\sqrt{p(z')\sec(K_1 z'')}$$
$$\times\operatorname{sech}\{\sec(K_1 z'')[\tau-\Lambda(z'')]\}$$
$$\times\exp\{i[C(z')t^2+\Phi(z'',\tau)]\}. \tag{18}$$

The presence of the dynamical chirp shifts the chirp-reversal location slightly away from z_c. Just after chirp reversal, we notice that the pulse seems to broaden, as is clearly seen in Fig. 5. Hence, the pulse needs to be retrieved at this point. With the help of a normal dispersive element such as grating, the original pulse can be recovered [19].

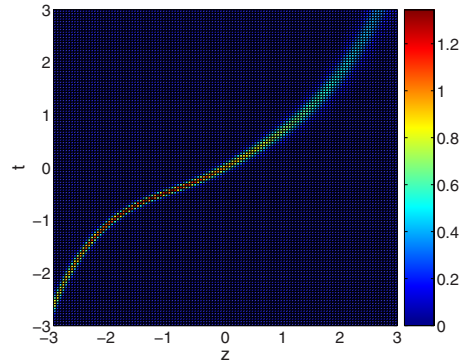

FIG. 5. (Color online) Pulse propagation having sinusoidal velocity profile. The plot shows broadening after chirp reversal.

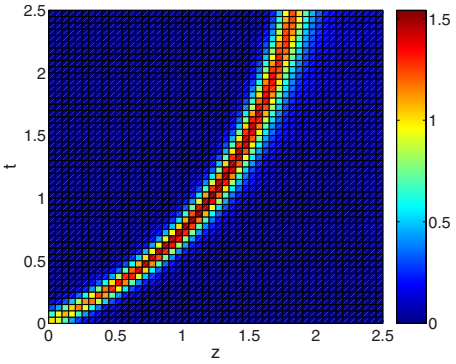

FIG. 6. (Color online) Soliton pulse acceleration with parameter $K_1<0$ implying an expulsive oscillator scenario.

In contrast to the above example, if we consider $K_1<0$, we obtain $\delta=[K_1-C^2(0)]^{1/2}$, which again leads to the same dispersion profile as that of the previous example, but with the pulse velocity $v(z'')=A_0\cosh(K_0z'')$. Figure 6 shows pulse dynamics for $K_1<0$. The expression for the soliton profile in this case is

$$q(z,t) = a(z)\sqrt{p(z')\mathrm{sech}(K_1z'')} \times \mathrm{sech}\{\mathrm{sech}(K_1z'')[\tau-\Lambda(z'')]\} \times \exp\{i[C(z')t^2+\Phi(z'',\tau)]\}. \quad (19)$$

It is interesting to observe that, compared with the previous case, pulse broadening is significantly reduced for the same parameter values.

Soliton bound states. Starting from Eq. (1) without tailoring the dispersion profile, we proceed to obtain self-similar solutions assuming the ansatz solution of the type

$$q(z,t) = \sqrt{A(z)}F\{A(z)[\tau-\Gamma(z)]\}\exp[G(z)+i\Phi(z,t)]. \quad (20)$$

The parameters appearing in Eq. (20) can be straightforwardly evaluated from Eqs. (11)–(13) and the soliton profile can be obtained from Eq. (14).

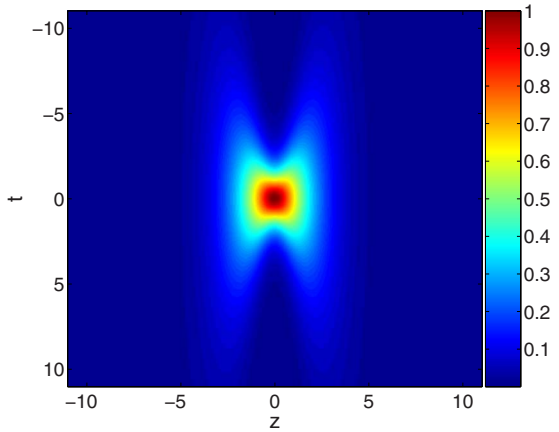

FIG. 7. (Color online) Soliton bound state in a medium with two dispersion regimes.

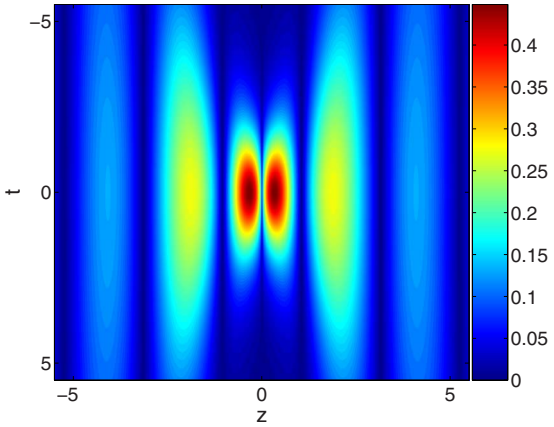

FIG. 8. (Color online) Multiple soliton bound state with oscillatory gain or loss.

Below, we explicate some examples of spatial bound states of solitons, arising from interplay of GVD, nonlinearity, and gain or loss. Figure 7 depicts a two-soliton bound state. This arises in a medium, where both anomalous and normal dispersion regimes are smoothly connected. In the presence of periodic gain or loss one observes modulation in the bound-state profile as is shown in Fig. 8.

This multisoliton bound state shows different behavior as compared to the two soliton one. The intensity profile has local minima as $z=0$. For the soliton bound state the origin corresponded to a maximum. The intensity modulations show multiple peaks and wider temporal variations for the former case. These can be controlled through GVD.

In conclusion, we have obtained exact soliton solutions exhibiting chirp reversal, while retaining their original profile, crucial for pulse recovery in fiber optics. Two different soliton sectors differing in propagation behavior, but with identical dispersion profiles, are analytically exhibited. We have outlined a general formalism for obtaining self-similar solutions of the nonlinear Schrödinger equation, in the presence of distributed coefficients, from which earlier scenarios follow as special cases [20]. It is shown that, this nonlinear system, involving pulse propagation with group velocity dispersion, variable nonlinearity, variable gain, exactly decouples into a elliptic function equation and a Schrödinger eigenvalue problem. This opens up a number of possibilities to take into account a wide class of distributed scenarios, in close conformity with the experimentally achievable situations. This incorporates a number of special cases dealt earlier, in the context of pulse compression. We find that, apart from compression, one can achieve control over the pulse velocity, pulse profile, through interplay of group velocity dispersion, nonlinearity, gain or loss. Formation of soliton bound states in a medium with GVD alternating between normal and anomalous dispersion is discussed. In the presence of the oscillatory gain or loss profile, we find the multiple bound-state structure.

The authors acknowledge many useful discussions with Professor G. S. Agarwal.

[1] G. P. Agrawal, *Nonlinear Fiber Optics* (Academic, San Diego, CA, 2001).
[2] A. Hasegawa and Y. Kodama, *Solitons in Optical Communications* (Oxford University Press, Oxford, 1995).
[3] M. J. Ablowitz and Z. H. Musslimani, Phys. Rev. E **67**, 025601(R) (2003).
[4] J. D. Moores, Opt. Lett. **21**, 555 (1996).
[5] V. I. Kruglov, A. C. Peacock, and J. D. Harvey, Phys. Rev. Lett. **90**, 113902 (2003).
[6] T. S. Raju, P. K. Panigrahi, and K. Porsezian, Phys. Rev. E **71**, 026608 (2005).
[7] L. F. Mollenauer, R. H. Stolen, J. P. Gordon, and W. J. Tomlinson, Opt. Lett. **8**, 289 (1983).
[8] E. M. Dianov, P. V. Mamyshev, A. M. Prokhorov, and S. V. Chernikov, Opt. Lett. **14**, 1008 (1989).
[9] M. L. Quiroga-Teixeiro, D. Anderson, P. A. Andrekson, A. Bernson, and M. Lisak, J. Opt. Soc. Am. B **13**, 687 (1996).
[10] R. Driben and B. A. Malomed, Phys. Lett. A **301**, 19 (2002).
[11] O. Solgaard, J. E. Ford, H. Fujita, and H. P. Herzig, IEEE J. Sel. Top. Quantum Electron. **8**, 1 (2002).
[12] S. P. Burtsev, A. V. Mikhailov, and V. E. Zakharov, Theor. Math. Phys. **70**, 227 (1987).
[13] V. N. Serkin, A. Hasegawa, and T. L. Belyaeva, Phys. Rev. Lett. **92**, 199401 (2004).
[14] S. Kumar and A. Hasegawa, Opt. Lett. **22**, 372 (1997).
[15] S. K. Turitsyn *et al.*, C. R. Phys. **4**, 145 (2003).
[16] I. Gabitov and S. K. Turitsyn, JETP Lett. **63**, 861 (1996); I. R. Gabitov and S. K. Turitsyn, Opt. Lett. **21**, 327 (1996).
[17] R. Atre, P. K. Panigrahi, and G. S. Agarwal, Phys. Rev. E **73**, 056611 (2006).
[18] H. Hancock, *Theory of Elliptic Functions* (Dover, New York, 1958); M. Abramowitz and I. Stegun, *Handbook of Mathematical Functions* (National Bureau of Standards, U.S. GPO, Washington, DC, 1964).
[19] P. A. Belanger and N. Belanger, Opt. Commun. **117**, 56 (1995).
[20] V. I. Kruglov, A. C. Peacock, and J. D. Harvey, Phys. Rev. E **71**, 056619 (2005); T. Soloman Raju, P. K. Panigrahi, and K. Porsezian, *ibid.* **72**, 046612 (2005); V. I. Kruglov and J. D. Harvey, J. Opt. Soc. Am. B **23**, 2541 (2006).